

Numerical Simulation of Ice Melting Near the Density Inversion Point under Periodic Thermal Boundary Conditions

A. Arid¹, T. Kousksou¹, S. Jegadheeswaran², A. Jamil³, Y. Zeraouli¹

Abstract: A two-dimensional numerical model has been developed to investigate the phase-change of ice near 4 °C in a rectangular cavity. The enthalpy-porosity model is reformulated in terms of conservation equations of mass, momentum and heat to account for the evolution the solid/liquid interface. Constant and time-dependent (with sinusoidal law) temperature boundary conditions are considered. Results confirm the possibility to control the typical dynamics of ice melting in a square cavity near the density inversion point by means of a wall temperature which varies in time (with given amplitude and frequency).

Keywords: Numerical analysis; Natural convection; Cyclic ice melting; Phase Change Materials.

Nomenclature

a	Carman-Kozney coefficient
C_p	specific heat capacity (J/kg.K)
f	liquid fraction
g	acceleration due to gravity (m/s ²)
h	sensible enthalpy, $h = C_p(T - T_m)$ (J/kg)
H	height (m)
k	thermal conductivity (W/ (m K))
L	latent heat of melting (J/kg)
Nu	Nusselt number, $Nu = -\frac{1}{T_H - T_C} \int_0^W \frac{\partial T}{\partial x} \Big _{x=0} dy$

¹ Laboratoire des Sciences de l'Ingénieur Appliquées à la Mécanique et au Génie Electrique (SIAME), Université de Pau et des Pays de l'Adour – IFR – A. Jules Ferry, 64000 Pau France

² Mechanical Engineering Area, Tolani Maritime Institute, Induri, Talegaon-Chakan Road, Pune 410 507, India

³ École Supérieure de Technologie de Fès, Université Sidi Mohamed Ibn Abdelah Route d'Imouzzer BP 2427.

p	pressure (N/m ²)
Pr	Prandtl number, $Pr = \frac{\nu_l}{\alpha_l}$
Ra	Rayleigh number, $Ra = \frac{g \cdot \gamma \cdot T_H - T_C ^b H^3}{\alpha_l \cdot \nu_l}$
t	time (s)
T	temperature (K)
u	component of velocity (m/s)
x, y	cartesian coordinates (m)
W	width (m)

Greek symbols

α	thermal diffusivity (m ² /s)
λ	under-relaxation factor
ν	kinematic viscosity (m ² /s)
ρ	density (kg/m ³)
μ	dynamic viscosity (kg/(m s))

Subscripts

l	liquid phase
s	solid phase
max	density maximum
m	melting
H	hot wall
ref	reference
i, j	direction index

Superscripts

m	previous iteration
$m + 1$	current iteration

1 Introduction

The problem of solid-liquid phase change, in particular ice melting/freezing has been the subject of many experimental and numerical investigations [Virag et al. (2006); Kim et al. (2008); Kousksou et al. (2010); Fukusako and Yamada (1993)].

This is due to the importance of this phenomenon in many applications, such as ice thermal storage techniques for air-conditioning, the ice production, etc. [Gong and Mujumdar (1996); Kousksou et al. (2008)].

The solid-liquid transition provides also a suitable technique for controlling temperature in systems, which are subjected to periodic heating. This process allows, for periodic heating, the conversion of temperature oscillations into oscillations of the melting interface, with a significant damping of the perturbation. Furthermore, the energy stored during melting can be recovered during freezing, with significant energetic opportunities. Semma et al [Semma et al. (2007)] considered investigations of convection with and without phase change submitted to modulated thermal boundary conditions applied to crystal growth cavities.

In the literature, Bransier [Bransier (1979)] seems to be the first who studied a system undergoing alternate processes of melting and freezing. He analyzed the problem of cyclic latent heat thermal storage both for slabs and hollow cylinders, by means of one-dimensional conduction model. Bardon et al. [Bardon et al. (1979)] performed the first experimental study on the periodic heat transfer for a vertical slab of PCM. A periodic phase change process dominated by heat conduction has been investigated numerically and experimentally by Casano and Piva [Casano and Piva (2002)]. In the experiments, a plane slab of phase change material was periodically heated from above. The comparison between the numerical predictions and experimental results showed good agreement. Elsayed [Elsayed (2007)] studied the melting of encapsulated ice for cold thermal energy storage. The influence of convection heat transfer as well as coolant fluid temperature under constant and cyclic variation with time has been investigated.

More of the works mentioned above have not considered the natural convection during the melting process, since the phase change process is dominated by the heat conduction. It is well known that natural convection plays an important role, especially in the melting process. Natural convection increases the heat transfer rate and thus, the melting rate, which in turn affects the shape and the motion of the solid-liquid interface [Gobin and Le Quéré (2002); El Ganaoui et al. (1999); El Ganaoui and Bontoux (1998); El Ganaoui et al. (2002); Kim and Kaviany (1992)].

The existence of the moving interface introduces a non linear behavior to the phase change problems and causes a lot of computational difficulties in the seeking of solution. We can also note that for the most phase change materials (PCMs), the density of the melt varies linearly with temperature. Unlike normal liquid PCMs, pure water exhibits maximum density near 4°C at atmospheric pressure. In such case, the problem becomes even more complex because the assumptions that the density varies linearly with temperature cannot be applied.

Numerical and experimental works involving maximum density and thermal natural convection can be found in the works of Braga and Viskanta [Braga and Viskanta (1992)], Kowalewski and Rebow [Kowalewski and Rebow (1999)] and Oosthuizen [Oosthuizen (2001)]. They analyzed the effect of the maximum density on water solidification in a rectangular cavity. Tsai et al. [Tsai et al. (1998)] presented a numerical work exploring the effect of the maximum density on laminar flows in tubes with internal solidification, involving mixed convection. Rieger and Beer [Rieger and Beer (1986)] investigated the effects of density anomaly on the melting process of ice inside a horizontal cylinder.

In relation to the numerical aspect of melting driven by natural convection problems, various geometries and solution methods have been considered. Fukasako and Yamada [Fukasako and Yamada (1993)] have presented an extensive summary of work concerning the analytical and numerical methods for freezing and melting problems, freezing of water and ice melting with and without convective flow. Examples of the experimental studies can be found in the works of Benard et al. [Benard et al. (1985)], Wolff and Viskanta [Wolff and Viskanta (1987)]. In the literature, two main approaches are used for numerical simulation of the phase change processes (i) fixed-domain formulation and (ii) variable-domain formulation. The former is used in the enthalpy formulation, in which a fixed grid is laid over the entire PCM domain and the latent heat release/absorption at the interface is accounted for by introducing a source term in the energy equation; while the latter is primarily adopted for the one immobilizing the moving interface via a suitable coordinate transformation and then solving for temperature distributions in the solid and liquid regions, separately. A review of numerical formulation of phase change processes is given by Jana et al. [Jana et al. (2007)].

In the literature, Ho and Chu [Ho and Chu (1993); Ho and Chu (1994)] seems to be the first who studied numerically a periodic melting in a rectangular enclosure with an oscillatory heated-wall temperature. They adopted a stream function-vorticity-temperature formulation to track the position of the liquid-solid interface during ice melting in a rectangular enclosure. They found a steady periodic melting regime arises following a period of transient oscillatory melting. Moreover, the heat transfer rates at the vertical heated and cooled walls as well as the melting rate exhibit a regular temporal oscillation at a frequency equal to the imposed wall temperature perturbation but with phase difference.

The main objective of the present study is to investigate the heat transfer characteristics of the natural-convection dominated melting process of ice from a vertical wall modulated with time-dependent sinusoidal surface temperature within a square enclosure via the enthalpy formulation. This is aimed at exploring the feasibility of controlling the melting heat transfer in an ice-filled enclosure by means of time

periodic perturbation of the wall temperature.

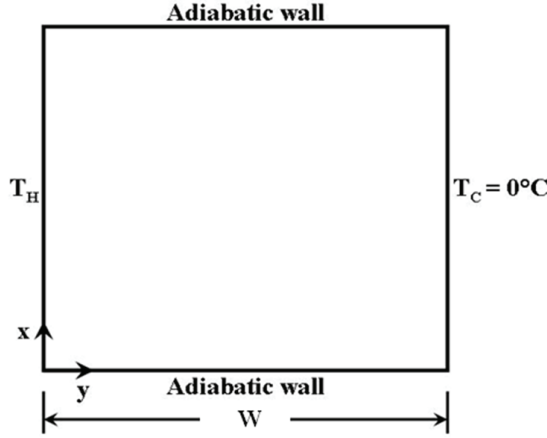


Figure 1: Computational domain for natural convection of water and ice melting with periodic boundary condition.

2 Governing equations

A generic representation of the analyzed geometry is presented in Fig.1. Flow in the melt region induced by natural convection is modeled by the incompressible Navier-Stokes equations. We assume that the flow is laminar and has no viscous energy dissipation. The conservation of mass and momentum equations are

$$\frac{\partial u_i}{\partial x_i} = 0 \quad (1)$$

$$\rho_l \frac{\partial u_i}{\partial t} + \rho_l u_j \frac{\partial u_i}{\partial x_j} = \frac{\partial}{\partial x_j} \left(\mu \frac{\partial u_i}{\partial x_j} \right) + g_i (\rho_l - \rho_{ref}) - \frac{\partial p}{\partial x_i} + A u_i \quad (2)$$

$$\frac{\partial (\rho_l h)}{\partial t} + u_j \frac{\partial (\rho_l h)}{\partial x_j} = \frac{\partial}{\partial x_j} \left(k \frac{\partial T}{\partial x_j} \right) + S \quad (3)$$

The buoyancy forces $g_i (\rho_l - \rho_{ref})$ are defined relative to some reference state ρ_{ref} . This means that p is the so-called motion pressure. To account for the latent heat effect in the phase change, occurring over a finite range of temperatures or at a fixed temperature, the general enthalpy method [Swaminathan and Voller (1992); El Ganaoui et al. (2002)] is adopted.

In the right hand side of the energy equation (3) we account for latent enthalpy transfer during phase change through the source term S , which is expressed as,

$$S = -L \frac{\partial(\rho f)}{\partial t} - u_j L \frac{\partial(\rho f)}{\partial x_j} \quad (4)$$

The present formulation is one-domain method, wherein the same set of equations is used for both solid and liquid. The material in the cavity is regarded as a porous medium with porosity varying with liquid fraction through Carman-Kozeny's law [Kim et al. (2008)]. The constant a in the source term of the momentum Equations has the form,

$$A = -\frac{C(1-f)^2}{f^3+q} \quad (5)$$

where C and q are two constants chosen to ensure driving the velocities to zero in the solid, while maintaining a convergent algorithm.

According to the above assumptions the liquid density is variable only on the last term of Eq. (2) and it was approximated by the Gebhart-Mollendorf formula [Gebhart and Mollendorf (1977)], which takes into account the water density inversion phenomenon

$$\rho_l = \rho_{\max} \left[1 - \gamma |T - T_{\max}|^b \right] \quad (6)$$

where $\rho_{\max} = 999.72 \text{ kg/m}^3$, $\gamma = 9.97 \times 10^{-6} \text{ K}^{-b}$, $T_{\max} = 4.29^\circ\text{C}$ and $b = 1.895$.

3 Numerical solution procedure

A structured grid of $N \times M$ control volumes for scalar variables (p , h) has been used, where as a staggered grid in the x and y direction has been employed to compute the velocity u_i . Each equation is integrated on a control volume centered at a node of the main variable of the equation. Second order accuracy is retained for quadratures, source terms and diffusion terms. Convective fluxes are approximated with the Power Law scheme. Time discretization is fully implicit (Euler Backward). Nonlinearity and coupling between the various equations are handled by the SIMPLEC algorithm [Doormaal and Raithby (1985)]. The momentum, pressure correction and temperature are solved sequentially using the modified strongly implicit procedure (MSIP) of Schneider and Zedan [Schneider and Zedan (1981)]. To improve the rate of convergence, under relaxation is introduced by means of a pseudo-transient scheme based on the E-factor formulation [Doormaal and Raithby (1985)].

The energy equation is non linear due to the presence of latent enthalpy content in the source terms arising from phase change. The process for handling this problem is largely described in Ref. [Raithby et al. (1986)].

At each outer iteration, the liquid fraction is updated from the values at the previous outer iteration (m) through the formula:

$$f_P^{m+1} = f_P^m + \lambda \frac{\Delta t a_p^{h,m}}{\rho L \Delta V} h_P^m \quad (7)$$

and

$$\begin{aligned} f_P^{m+1} &= 1 \quad \text{if } f_P^m \geq 1 \\ f_P^{m+1} &= 0 \quad \text{if } f_P^m \leq 0 \end{aligned} \quad (8)$$

where a_p^h stand for the central coefficients of the discretized energy equation and the unsteady term coefficient respectively and λ is the under-relaxation factor. At a given time step, the position of the phase front is obtained from the solution of the liquid fraction field by a linear interpolation of the contour line when $f = 0.5$.

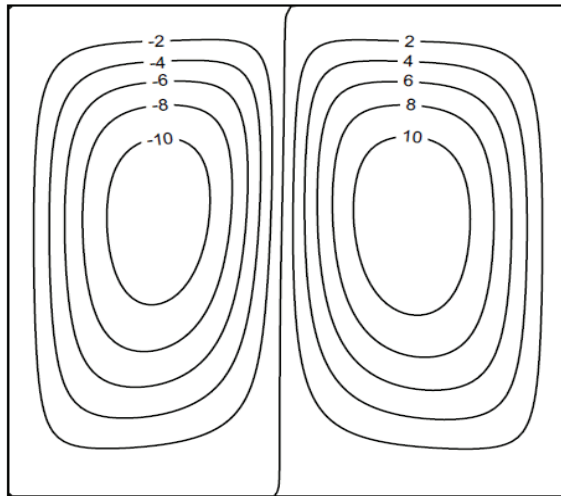
The process is repeated until a relative difference between two consecutive iterations of the sensible enthalpy is less than a given tolerance, i.e.

$$|h^{m+1} - h^m| / h^m < 10^{-5} \quad (9)$$

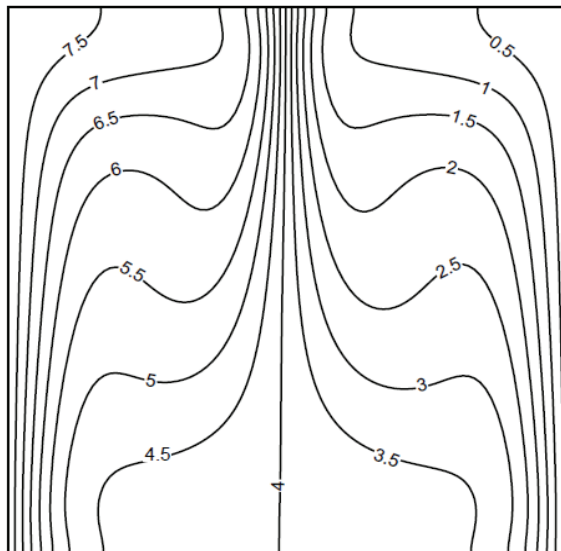
Global convergence is achieved when the mass balance is verified in all control volumes within a prescribed value (typically 10^{-9}) and when the residual values of the different values of the different equations are sufficiently low (typically 10^{-10})

4 Model verification

To validate the fluid flow problem without phase change the natural convection of water in a closed square cavity (see Fig.1) at a temperature large than its maximum density is analyzed. At time $t = 0$, the left boundary is suddenly brought to the temperature $T_H = 8^\circ\text{C}$, whereas the right boundary remains at $T_H = 0^\circ\text{C}$. The results obtained are given in Fig.2, in terms of streamlines and temperature contours. The flow patterns describe two symmetrical cells rotating in opposite directions, as expected for this physical situation, where the fluid temperature range is centered in the density inversion point. It is natural that the streamlines and isotherms display certain symmetries about the central vertical line. Each sidewall generates an identical upward buoyancy force and therefore, a two-cell flow is obtained with fluid flowing down the middle of cavity [Leonard (1986); Doormaal and Raithby (1985); Hossain and Rees (2005); Osorio et al. (2004)].



(a)



(b)

Figure 2: Natural convection of water for $T_H=8^\circ\text{C}$, $R_{aH}=1.03\times 10^7$ and $Pr=13$ (a) stream function (b) temperature fields.

The distribution of dimensionless temperature in the middle plane of the cavity ($X^* = x/W = 0.5$) is compared with the experimental data of Inaba and Fukuda [Inaba and Fukuda (1984)], as well as with the numerical predictions of Lin and Nansteel [Lin and Nansteel (1987)]. The comparison is presented in (Fig.3). We can note that the present results are in good agreement with the results reported by Lin and Nansteel [Lin and Nansteel (1987)]. Nevertheless, there is a significant discrepancy between the present results and the experimental data. According to Osorio et al. [Osorio et al. (2004)], the experimental data of Inaba and Fukuda [Inaba and Fukuda (1984)] suggest a profile more typical of a un-cellular flow, with maximum temperature gradients near the isothermal walls and a single central region where the temperature is almost uniform. This is not the expected flow pattern for the physical problem herein considered.

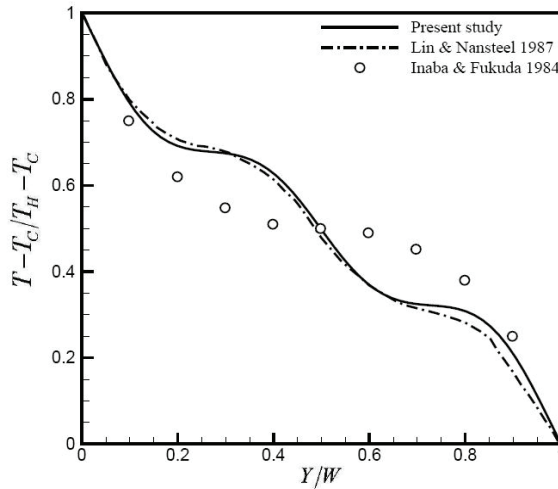


Figure 3: Comparison of predicted temperature distribution of the present model with literature data $T_H=8^\circ\text{C}$, $Ra_H=1.03 \times 10^7$, $Pr=13$ and $x/W = 0.5$.

To verify the model in case of coupled melting process and natural convection near 4°C , the melting problem of a vertical ice layer is solved. In this case, the melting process occurs inside a rectangular cavity, in the presence of the horizontal temperature gradients (Fig. 4). At time $t = 0$, half of the material volume is in solid state (ice), while the other half is in liquid state (water). Now, the western wall is abruptly heated to the temperature $T_H = 8^\circ\text{C}$ and maintained at this temperature thereafter. Eastern wall is maintained at melting temperature. The northern and southern walls are adiabatic. Initially, all the volume of the testing substance is set at its melting temperature. For this problem, the grid defined on the computational

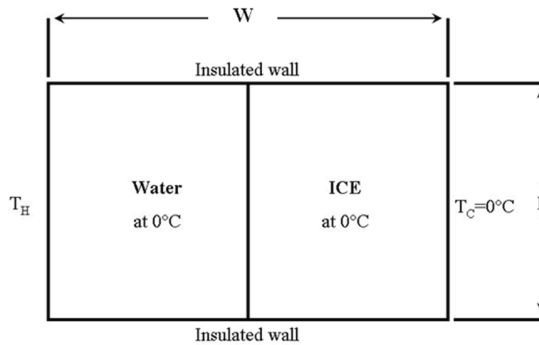


Figure 4: Computational domain of vertical ice layer melting process.

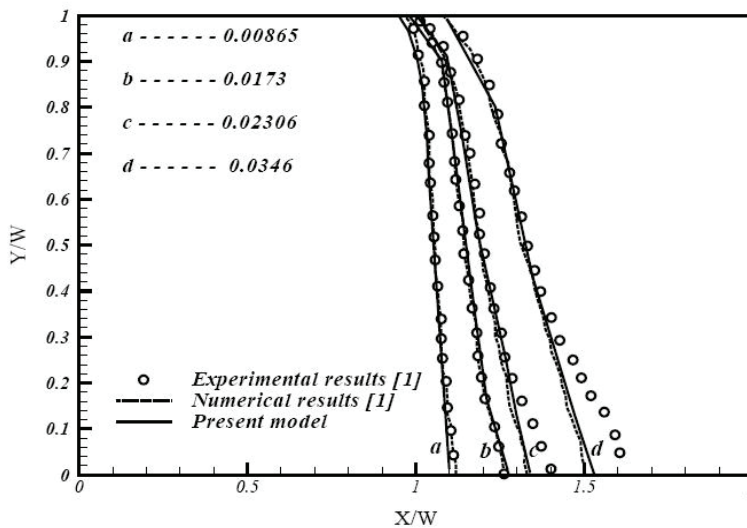


Figure 5: Comparison of predicted melting front location at selected times of the present model with the results of Ref. [1].

domain is spaced irregularly to obtain a better solution of temperature and velocity gradients near the liquid -solid interface.

The predicted liquid-solid interface positions are compared with those determined experimentally and numerically [Virag et al. (2006)] in Fig.5. As may be observed at the beginning of the melting process, the numerical results are in good agreement with the experiment data and the numerical results reported by Virag et al [Virag et al. (2006)]. Nevertheless, at the end of the process, there is certain discrepancy,

especially at the bottom of the cavity. The main reason is the difficulty maintaining the vertical wall at a desired temperature. Despite these deficiencies, the predicted interface shapes are qualitatively correct and the obtained results confirm the validity of the adopted numerical model.

5 Phase change with periodic boundary conditions

In this section, the melting of ice under cyclic variation of wall temperature is investigated. The physical configuration of the melting problem under consideration is the same square enclosure shown in Fig.1. Initially, ice in the square enclosure is at its phase change temperature. The upper and lower walls are assumed to be adiabatic. At time $t = 0$, the left boundary is suddenly brought to a sinusoidal variation of temperature with time. The prescribed sinusoidal temperature has a period of 80 min and amplitude of 2°C and the temperature oscillates about a mean value of 4°C as shown in Fig.6. It should be mentioned here that at time $t = 0$, the sine function starts with the mean value of the temperature oscillation.

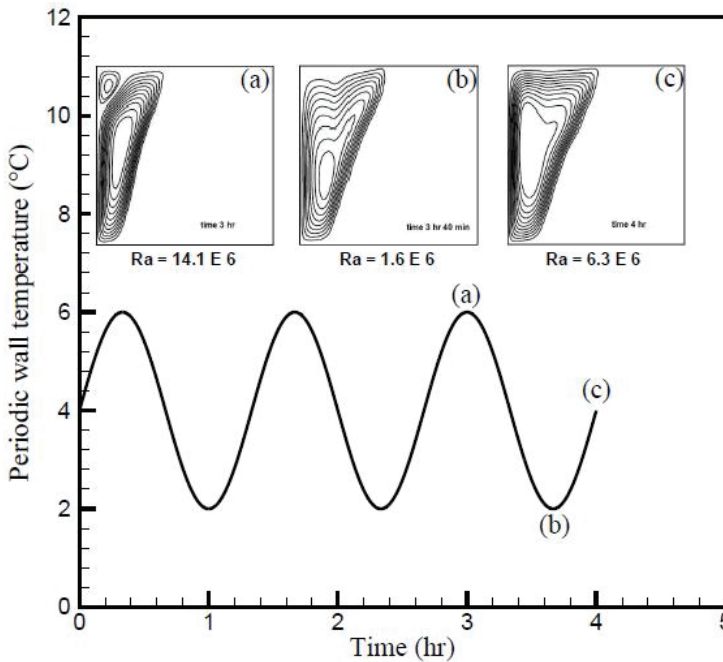


Figure 6: Time evolution of the periodic wall temperature and flow pattern over the oscillation period.

In Fig.6, we have plotted the periodic wall temperature versus time and the flow pattern at different instant. At early times, the heat transfer in the melt zone is predominated by conduction. After a while, the thickness of the melt layer becomes large enough so that natural convection is triggered. As time passes, the melt layer expands and natural convection becomes the prevailing mechanism of heat transfer inside the liquid region. The intensity and the direction of the buoyancy driven flows are dependent on the value of the imposed sinusoidal temperature. For the cases (b) and (c) when sinusoidal temperature becomes equal to 2°C or 4°C, we show a unicellular flow pattern with a larger melt region in the top part of the cavity. High melting occurs at the top of the solid-liquid interface where warm and denser fluid impinges after being heated by the hot wall. For the case (a) when sinusoidal temperature becomes equal to 6°C, a dual cell flow pattern occurs. As water with maximum density is located somewhere in the melt region, two counter-rotating recirculation bubbles have established themselves. Since the point of maximum density is closer to the square cavity than to the interface, the counterclockwise cell should be close to the hot wall.

For a given sinusoidal wall temperature, the temperature of water at a point ($x=W/2$, $y=H/2$) near the wall heated versus the time is presented by Fig.7.

Three Rayleigh numbers have been tested to check the influence of the sinusoidal wall temperature on the heat transfer inside the square cavity. It has been noticed that, from numerical experiments, the temperature of a given point oscillates (sinusoidal mode) with the wall temperature. We observe that for $1.6 \text{ E}6 < \text{Ra} < 14.1 \text{ E}6$, the temperature profile at this point is adjacent to the wall temperature. However, the amplitude of the PCM temperature increases with the Rayleigh number value.

The effect of the flow pattern on the temporal variation of the molten volume fraction is depicted in Fig.8. The melting rate is maximum for $\theta=6^\circ\text{C}$ and minimum for $T_H=2^\circ\text{C}$. Also, for three temperature 2°C, 4°C and 6°C, this fraction increases almost linearly with time once the convective motion is well established throughout the melt. The molten volume fraction corresponding to the sinusoidal temperature is compared in Fig.8 with the molten volume fraction in the case of constant temperature $T_H = 4^\circ\text{C}$ which is the mean temperature value of the periodic variation. It is seen from this plots that the liquid fraction for constant temperature $T_H=4^\circ\text{C}$ is in the neutral position of oscillation of the cyclic molten volume fraction curve. This is due to the fact that the net heat input to the square cavity is the same in the two cases.

The timewise variations of the average Nusselt number at the heated wall are depicted in Fig.9. The Nusselt number, indicates the capacity of heat transfer in dimensionless form. Dimensionless local Nusselt number at hot side can be defined

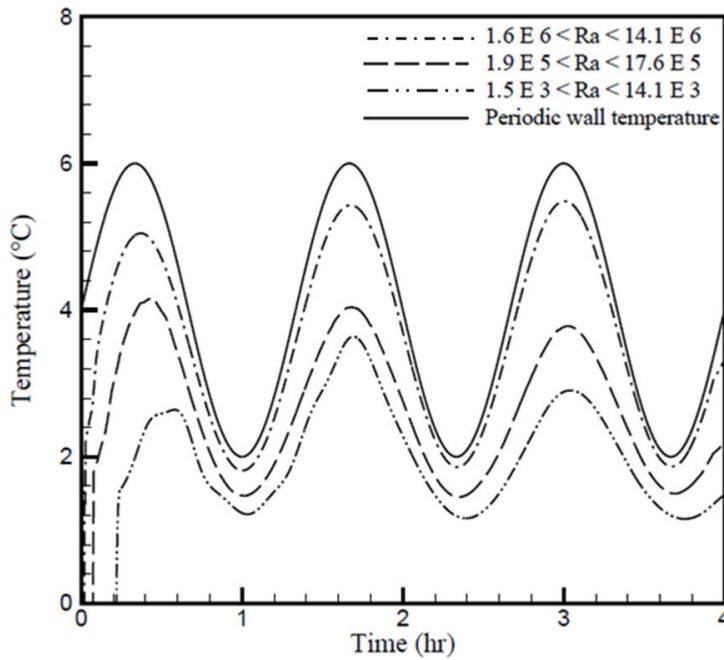


Figure 7: Comparison of water temperature near the heated wall for the different Rayleigh numbers.

as below:

$$Nu = -\frac{1}{T_H - T_C} \int_0^w \left. \frac{\partial T}{\partial x} \right|_{x=0} dy \quad (10)$$

The Nusselt number was calculated from the converged temperature field at each time step. The results display a rapid decrease in the heat transfer rate at the early stages of melting. This behavior results from transient heat conduction. As soon as natural convection sets in the liquid region, the heat transfer rate starts increasing. This is clearly shown for the case with $T_H=6^\circ\text{C}$ and, to a lesser extent, for the case with $T_H=4^\circ\text{C}$. In both the cases, a clockwise recirculating eddy establishes itself along the phase front, yielding large temperature gradients and therefore enhanced heat transfer rates. For the case with $T_H=2^\circ\text{C}$, the average Nusselt number stays nearly constant until the natural convection sets in the liquid region. This is due to the fact that the warm water tends to enter the space above and below the interface. That is why the ice melting is nearly uniform from all sides. In the case

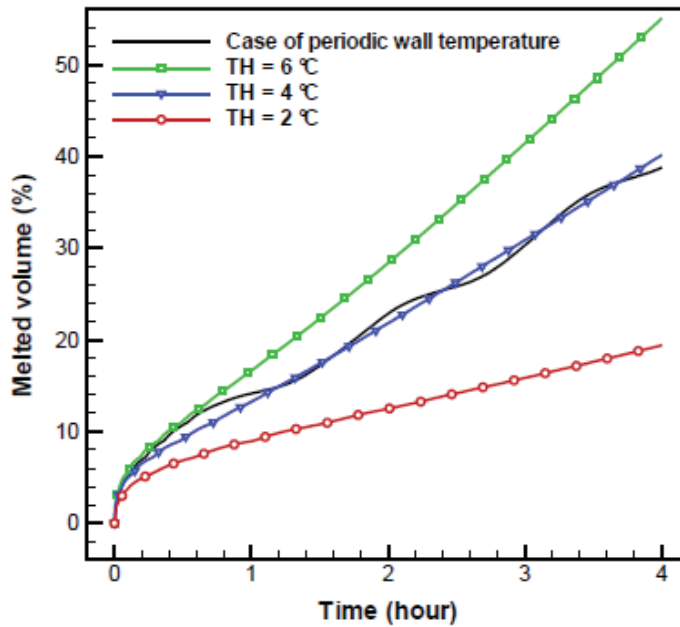


Figure 8: Total molten volume fraction under periodic and constant wall temperature for cases $T_H=6, 4$ and 2°C .

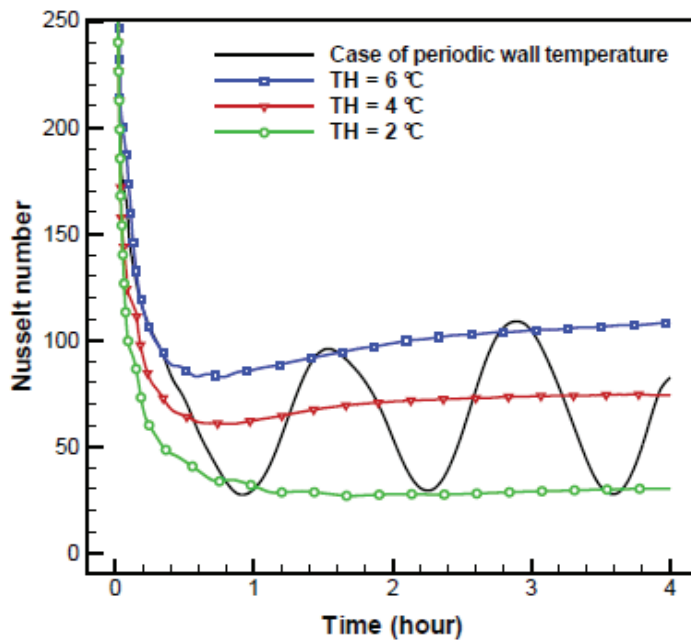


Figure 9: Time evolution of the average Nusselt number at the hot wall, for different wall temperatures.

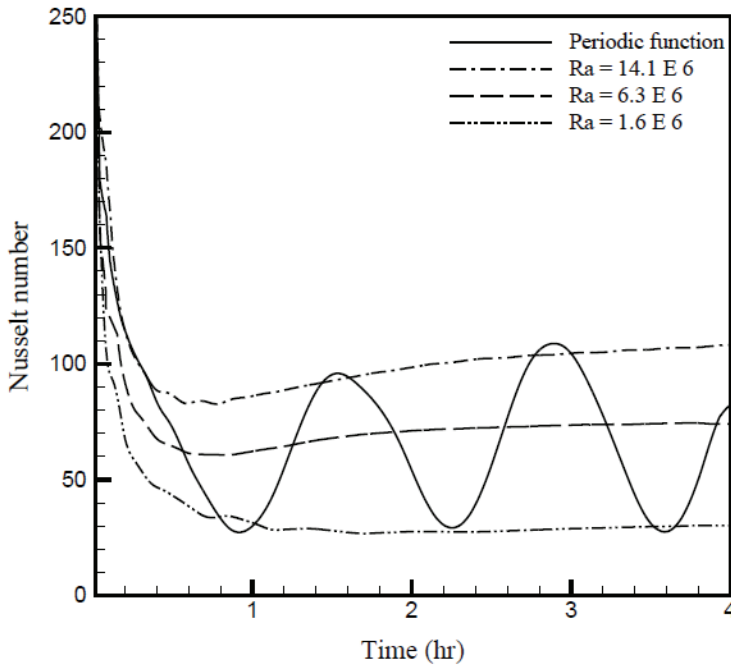


Figure 10: Time evolution of the average Nusselt number at the hot wall, for different Rayleigh numbers.

of periodic wall temperature, the average Nusselt number decreases rapidly during the first stages of melting. As soon as natural convection sets in the melt, the average Nusselt becomes to oscillate. This is due to the periodic melting of ice in the square cavity. We note that the average Nusselt number in the case of constant wall temperature $T_H=4^\circ\text{C}$, is in the neutral position of oscillation of the periodic average Nusselt number. We can also note that the maximum and minimum values of the periodic average Nusselt number corresponds respectively to the average Nusselt number of the wall temperatures $T_H=6^\circ\text{C}$ and $T_H=8^\circ\text{C}$.

In case of periodic wall temperature, we have presented timewise variations of the average Nusselt number for three Rayleigh numbers (see Fig.10). It is clear that the oscillation of the Nusselt number is more intensive for $1.6\text{E}6 < \text{Ra} < 14.1\text{E}6$. We can also note that the amplitude of the average Nusselt number decreases with decrease in Rayleigh number. Using the higher Rayleigh number, the liquid region behaves as a damper.

6 Conclusions

We have considered the melting of ice in a square enclosure near the density inversion point in the framework of a numerical approach.

Resolution of the natural convection of water near the density inversion point has been first checked by comparison with literature data. The problem of a vertical ice layer in the presence of a horizontal temperature gradient has been also tested by comparison with previous experimental and numerical data.

We have found that the effect of an oscillating boundary temperature on the melting process of ice is more pronounced when the Rayleigh number is small. The liquid fraction in the system has been observed to oscillate in time with the imposed sinusoidal temperature. For the present problem, more extensive studies, especially experimental and with a wider range of the considered relevant parameters, are needed in future.

Acknowledgement: This work has been realized with the support of the Inter Universitaire Franco-Marocain committee in the framework of the integrated action VOLUBILIS n° MA/06/152).

References

Bardon, J.P.; Vrignaud, E.; Delaunay, D. (1979) : Etude expérimentale de la fusion et de la solidification périodique d'une plaque de paraffine. *Revue Générale and Thermique*, vol. 212-213, pp. 501-510.

Benard, C.; Gobin, D.; Martinez, F. (1985): Melting in rectangular enclosures: Experiments and numerical simulations. *Journal of Heat Transfer*, vol. 107, pp. 794-803.

Braga, S.L.; Viskanta, R. (1992): Transient natural convection of water near its density extremum in a rectangular cavity. *International Journal of Heat and Mass Transfer*, vol. 35, pp. 861-875.

Bransier, J. (1979): Storage périodique par chaleur latente : aspects fondamentaux liés à la cinétique des transferts. *International Journal of Heat and Mass Transfer*, vol. 22, pp. 875-883.

Casano, G.; Piva, S. (2002): Experimental and numerical investigation of the steady periodic solid-liquid phase-change heat transfer. *International Journal of Heat and Mass Transfer*, vol. 45, pp. 4181-4190.

Doormaal, J.P.; Raithby, G.D. (1985): An evaluation of the segregated approach for predicting incompressible fluid flows. *ASME Paper*, 85-HT-9.

Doormaal, J.P.; Raithby, G.D. (1985): An evaluation of the segregated approach

for predicting incompressible fluid flows. *ASME Paper*, pp. 11.

EL Ganaoui, M. ; Bontoux, P. ; Morvan, D. (1999) : Localisation d'un front de solidification en interaction avec un bain fondu instationnaire. *C. R. Acad. Sci. Paris, série Iib*, vol. 327, pp. 41-48.

EL Ganaoui, M.; Bontoux, P. (1998): An homogenisation method for solid-liquid phase change during directional solidification. *ASME, H.T.D., Numerical and Experimental Methods in Heat Transfer*, éd. R.A. Nelson, T. Chopin, S.T. Thynell, vol. 361, no. 5, pp.453-469.

EL Ganaoui, M.; Lamazouade, A.; Bontoux, P.; Morvan, D. (2002): Computational solution for fluid flow under solid/liquid phase change conditions, *Int. J. Computers and Fluids*, vol.31, pp. 539-556.

Elsayed, A.O. (2007): Numerical study of ice melting inside rectangular capsule under cyclic temperature of heat transfer fluid. *Energy Conversion and Management*, vol. 48, pp. 124-130.

Fukasako, S.; Yamada, M. (1993): Recent advances in Research on Water Freezing and Ice Melting Problems. *Experimental Thermal and Fluid Science*, vol. 6, pp. 90-105.

Gebhart, B.; Mollendorf, J.C. (1977): A new density relation for pure and saline water. *Deep Sea Research*, vol. 24, pp. 831-848.

Gobin, D.; Le Quééré, P. (2000): Melting from an isothermal vertical wall. *Computer Assisted Mechanics and Engineering Sciences*, vol.7-3, pp. 289-306.

Gong, Z.X.; Mujumdar, A.S. (1996): Enhancement of energy charge-discharge rates in composite slabs of different phase change materials. *International Journal of Heat and Mass Transfer*, vol. 39, pp. 725-733.

Ho, C.J.; Chu, C.H. (1993): Periodic melting within a square enclosure with an oscillatory temperature. *International Journal of Heat and Mass Transfer*, vol. 36, pp. 725-733.

Ho, C.J.; Chu, C.H. (1994): A simulation for multiple moving boundaries during melting inside an enclosure imposed with cyclic wall temperature. *International Journal of Heat and Mass Transfer*, vol. 37, pp. 2505-2516.

Hossain, M.A.; Rees, D. A. (2005): Natural convection flow of water near its density maximum in a rectangular enclosure having isothermal walls with heat generation. *Heat and Mass Transfer*, vol. 41, pp. 367-374.

Inaba, H.; Fukuda, T. (1984): Natural convection in a square cavity in regions of density inversion of water. *Journal of Fluid Mechanics*, vol. 142, pp. 363-381.

Jana, S.; Ray, S.; Durst, F. (2007): A numerical method to compute solidification and melting processes. *Applied Mathematical Modeling*, vol. 31, pp. 93-119.

Kim, C.J.; Kaviany, M. (1992): A numerical method for phase change problems with convection and diffusion. *International Journal of Heat and Mass Transfer*, vol. 35, pp.457-467.

Kim, M.C.; Choi, C.K.; Yoon, D.Y. (2008): Analysis of the onset of buoyancy-driven convection in a water layer formed by ice melting from below. *International Journal of Heat and Mass Transfer*, vol. 51, pp. 5097-5101.

Kousksou, T.; Bédécarrats, J.P.; Strub, F.; Castaing-Lasvignottes, J. (2008): Numerical Simulation of fluid flow and heat transfer in a phase change thermal energy storage. *International Journal of Energy Technology and Policy*, vol. 6, pp. 143-158.

Kousksou, T.; Ahmed, A.; Majid, J.; Zeraouli, Y. (2010): Numerical modeling of double- diffusive convection in ice slurry storage tank. *International Journal of Refrigeration*, vol. 33, pp.1550-1558.

Kowalewski, T.A., Rebow, M. (1999): Freezing of water in a differentially heated cubic cavity. *International Journal of Computational Fluid Dynamics*, vol. 11, pp. 193-210.

Leonard, B.P. (1979): A stable and accurate convective modeling procedure based on quadratic upstream interpolation. *Computational Methods in Applied Mechanics and Engineering*, vol. 19, pp. 59-98.

Lin, D.S.; Nansteel, M.W. (1987): Natural convection heat transfer in a square enclosure containing water near its density maximum. *International Journal of Heat and Mass Transfer*, vol. 30, pp. 2319-2329.

Oosthuizen, P.H. (2001): The development of convective motion in a bottom heated square enclosure containing ice and water. vol. 40 pp. 145-151.

Osorio, A.; Avila, R.; Cervantes, J. (2004): On the natural convection of water near its density inversion in an inclined square cavity. *International Journal of Heat and Mass Transfer*, vol. 47, pp. 4491-4495.

Raithby, G.D.; Galpin, P.F.; Doormaal, J.P. (1986): Prediction of heat and fluid flow in complex geometries using general orthogonal coordinates. *Numerical Heat Transfer*, vol. 9, pp. 125-142.

Rieger, H.; Beer, H. (1986): The melting process of ice inside a horizontal cylinder: effects of density anomaly. *Journal of Heat Transfer*, vol. 108, pp. 166-173.

Schneider, G.E.; Zedan, M. (1981): A modified strongly implicit procedure for the numerical solution field problems. *Numerical Heat Transfer*, vol. 4, pp. 1-9.

Semma, EL A.; Ganaoui, M.; Bennacer, R. (2007): Lattice Boltzmann method for melting/solidification problems. *C. R. Mecanique*, vol. 335, pp. 295-303.

Swaminathan, C.R.; Voller, V.R. (1992): General Enthalpy Method for Modeling

Solidification Processes. *Metallurgical Transactions B*, vol. 23, pp. 651-664.

Tsai, C.W.; Yang, S.J.; Hwang, G.J. (1998): Maximum density effect on laminar water pipe flow solidification. *International Journal of Heat and Mass Transfer*, vol. 41, pp. 4251-4257.

Virag, Z.; Zivic, M.; Galovic, A. (2006): Influence of natural convection on the melting of ice block surrounded by water on all sides. *International Journal of Heat and Mass Transfer*, vol. 49, pp. 4106-4115.

Wolff, F.; Viskanta, R. (1987): Melting of a pure metal from a vertical wall. *Experimental Heat Transfer*, vol. 1, pp. 17-30.

